



## Electrochemical degradation of dye on lead dioxide electrodeposited on stainless steel: effect of cyclic voltammetry parameters

Ines Elaissaoui, Hanene Akrouit\*, Latifa Bousselmi

Laboratory of Wastewater Treatment, Center of Water Research & Technology (CERTÉ), Borj Cédria PB 273, Soliman 8020, Tunisia, Tel. +216 79 325 044; email: [issaouines@yahoo.fr](mailto:issaouines@yahoo.fr) (I. Elaissaoui), Tel. +216 79 325 044; Fax: +216 79 325 802; email: [hanene.akrouit@yahoo.com](mailto:hanene.akrouit@yahoo.com) (H. Akrouit), Tel. +216 79 325 044; email: [latifa.bousselmi@certe.rnrt.tn](mailto:latifa.bousselmi@certe.rnrt.tn) (L. Bousselmi)

Received 1 August 2015; Accepted 29 November 2015

### ABSTRACT

The effect of cyclic voltammetry (CV) on electrochemical behavior of PbO<sub>2</sub> layer electrodeposited by pulsed method on stainless steel (AS30) has been studied. The field emission scanning electrons microscope and X-ray diffraction (XRD) were used to characterize the surface morphology and crystal structure of different electrodes with CV effect, respectively. The content of PbO<sub>2</sub> particles has been tuned by altering the cycle number, of CV through which the content of PbSO<sub>4</sub> also increased. It is related to reduction phenomena depending on electron transfer through the pores into β-PbO<sub>2</sub> layer. Electrochemical behavior of the prepared samples was investigated in 0.5 M H<sub>2</sub>SO<sub>4</sub> solution by CV and electrochemical impedance spectroscopy (EIS) techniques. EIS results revealed that the charge-transfer resistance significantly increased because the lead sulfate layer is more compact and the access of electrolyte ions to the internal layer is blocked. Anodic oxidation of solutions containing Amaranth as a dye model was studied to evaluate the use of these electrodes as anodes in environmental issue. After five cycle of CV, PbO<sub>2</sub> film becomes more resistive according to value of  $R_f$  and this may have a deleterious effect on the electrochemical degradation activity compared to that without CV treatment. Based on the obtained results, after electrolysis time of 5 h at acidic pH medium, the color and the chemical oxygen demand removals on PbO<sub>2</sub> electrode treated by 1 CV achieved nearly to 97 and 83%, higher than that without CV treatment (77 and 47%), respectively.

*Keywords:* Electrodeposition; Lead dioxide; Cyclic voltammetry; Stainless steel; Degradation

### 1. Introduction

Due to its low cost, ease for synthesis, and stability in acidic media, lead dioxide has attracted great interest in a wide range of technological applications such

as oxidation of organic materials in waste water treatment [1,2], sensors [3], energy storage devices such as batteries [4], and in super capacitors [5]. On the other hand, the use of stainless steel was selected as substrates for PbO<sub>2</sub> layer because of its inexpensive cost and good corrosive stability [6]. This choice is related not only to the sustainable development of

\*Corresponding author.

wastewater, but also to the reduction of the lead pollution to the environment [1].

Lead dioxide has been prepared by the chemical [7,8] and electrochemical methods [9,10], various electrochemical methods including CV [11], pulse current [12,13], constant potential [14], and constant current [15] techniques have been employed to synthesize  $\text{PbO}_2$ . Moreover, it has been found that electrochemical behavior of  $\text{PbO}_2$  depends on various parameters including particle size [16], morphology [17], and phase composition [18]. Morphology and particle size strongly influence the electrochemical activity of the materials [16] by affecting their active surface area [12] and interparticle contacts [19]. The electrodeposited  $\text{PbO}_2$  depends on various parameters such as type of the substrate nature (pure metal, alloy, etc.), the electrodeposition method used [11], and the synthesis conditions [20]. The composition and morphology of  $\text{PbO}_2$  affect also the electrochemical activity. It has been recognized that a porous structured  $\text{PbO}_2$  should give more active properties [21].

The oxidation mechanism pathway of organics is very complex. The principal oxidants that can be detected were important for understanding the degradation mechanism [22]. It is well known that the electrochemical activity of  $\text{PbO}_2$  electrodes depends largely on the composition of the film. The stability and electrocatalytic activity of the  $\text{PbO}_2$  anodes are expected to be improved to further satisfy the requirement of practical application.

The presence of lead sulfate in the production of positive active materials has many advantages [23] where it is produced using CV which is considered the most widely used technique for acquiring qualitative information about electrochemical reactions [24]. At the electrode surface, the ratio  $\text{PbO}_2/\text{PbSO}_4$  is related to the redox activity because the entry of electron is insured through the pores of  $\text{PbO}_2$  in order to reduce  $\text{PbSO}_4$  easily [25].

The main goal of the present contribution is to investigate the influence of CV action on the electrochemical activities of  $\text{PbO}_2$  deposited onto stainless steel. The structure and the morphology of obtained films after different cycle number of CV are characterized in ex-situ through X-ray Diffraction (XRD) and field emission scanning electron microscopy (FESEM) techniques. Electrochemical impedance spectroscopy (EIS) is also used to characterize the resistances and capacities of different films after electrochemical treatments. We tried to find a correlation between the performance of lead dioxide activity in the oxidation of organic compounds and the cycle number of CV used for anode treatment. The degradation efficiency of the Amaranth dye using different elaborate anodes is

investigated in terms of color and chemical oxygen demand (COD) removal.

## 2. Experimental and methods

### 2.1. Chemicals and instrumentation

$\text{Pb}(\text{NO}_3)_2$  (Panerac Quimica SA-99%),  $\text{HNO}_3$  (Sigma-Aldrich-95-97%) were prepared for deposition of  $\text{PbO}_2$  film. Sodium sulfate ( $\text{Na}_2\text{SO}_4$ , Sigma-Aldrich 99%) was used as supporting electrolyte (0.1 M) during the degradation. Sulfuric acid (Sigma-Aldrich-95-97%) is used for electrochemical treatment and for initial adjustment of pH (equal to 2) of samples solution. The dye pollutant is Amaranth (E123) (Sigma-Aldrich), azo dye, having a molecular formula  $\text{C}_{20}\text{H}_{11}\text{N}_2\text{Na}_3\text{O}_{10}\text{S}_3$  and a molar mass of  $606.48 \text{ g mol}^{-1}$ . The concentration of dye is fixed at 0.015 mM, in 0.1 M  $\text{Na}_2\text{SO}_4$ . Experiments were carried out at acidic pH medium applying current density of  $25 \text{ mA cm}^{-2}$  (with Thermo scientific EC300 XL power supply) with electrolysis time of 300 min. The discoloration of Amaranth was followed by UV-vis spectrophotometry analysis (Thermospectronic UV1) and the mineralization by measurement of COD was determining using the reactor digestion method based on the method of acidic oxidation by dichromate.

### 2.2. Electrode preparation

Before each deposition, the AS30 electrode was mechanically polished with abrasive papers (P 600 and P 1,200) and rinsed with water. For chemical pollution, submerged sulfuric acid (0.1 M) at  $50^\circ\text{C}$  was sonicated for 10 min. It was then rinsed with water for 5 min and sonicated in acetone for 2 min in order to remove any surface oxidized species in contact with air [26].

$\text{PbO}_2$  was directly synthesized by the pulsed current method on the surface of SS electrode from solution of 0.5 M  $\text{HNO}_3$  + 0.5 M  $\text{Pb}(\text{NO}_3)_2$ . For each electrode, 170 pulses (pulse height of  $30 \text{ mA cm}^{-2}$ , pulse width of 1 s at  $30 \text{ mA cm}^{-2}$ , and relaxation time of 5 s at zero current) were applied. All samples were carried out at the room temperature [27].

### 2.3. Surface characterization

The surface morphologies of  $\text{PbO}_2$  anodes were examined using a field emission scanning electrons microscope (FESEM Zeiss Supra 40). The crystalline structures of different anodes were examined by a X-ray diffractometer (DRX model X'Pert Pro, PANalytical) using  $\text{Cu K}\alpha$  ( $\lambda_1 = 1.5405980$ ).

#### 2.4. Electrochemical measurements

Electrochemical behavior of PbO<sub>2</sub> anodes was tested with a conventional three-electrode cell using a VoltaLab 40 PGZ301 potentiostat (Radiometer Analytical), connected with a computer that uses VoltaMaster 4.0 software for data. Cell using AS30/PbO<sub>2</sub> as anode, a Pt as counter electrode, and a saturated calomel electrode as reference electrode on the VoltaLab 40 PGZ301 potentiostat (Radiometer Analytical) connected with a computer that used VoltaMaster 4.0 software for data analysis. The cycle number of CV was varied from 1 to 30 in the potential region from 0.7 to 2.0 V at a scan rate 50 mV s<sup>-1</sup> in 0.5 M sulfuric acid.

EIS measurements were carried out at the open-circuit potential, the frequencies swept are undertaken from 100 kHz to 100 mHz by applying a sinusoidal signal of 5 mV amplitude. The experimental data from EIS diagrams were analyzed and fitted using the software, ZsimpWin3.2. Impedance spectra were recorded at the open-circuit potential after immersion of electrodes for 15 min in electrolyte solution, the active surface area of each electrode is equal to 4 cm<sup>2</sup>.

#### 2.5. Atomic absorption

Atomic Absorption Spectroscopy (Analyst 200 Perkin–Elmer) with graphite furnace (GFAAS) (HGA 900-Perkin Elmer) used to determining the concentration of lead ion from anodes into solution after electrolysis. Analysis with GFAAS was done according to standard method.

#### 2.6. Anodic oxidation of Amaranth dye

The electrolysis of aqueous solution containing Amaranth dye was carried out in a one-liter one-compartment Pyrex glass cell in which the AS30/PbO<sub>2</sub> anode was designed vertically and parallel to the stainless steel cathode, both of them have a surface of 4 cm<sup>2</sup>. Initial Amaranth (E123) dye concentration of 0.015 mM was used to examine the degradation over AS30/PbO<sub>2</sub> anodes which are pretreated by different cycle number of CV. The supporting electrolyte (Na<sub>2</sub>SO<sub>4</sub>) concentration was 0.1 M. The solution was kept at temperature of 25°C under stirring to ensure the efficiency of mass transfer. All experiments were carried out at electrolysis time of 300 min.

UV–vis absorption spectra of Amaranth solutions were recorded by spectrophotometry (Perkin–Elmer model) in the wave range of 400–600 nm. The mineralization by measurement of COD is determined by the dicromate reactor digestion method.

Experimentally, the discoloration efficiency or percentage of color removal during the treatment of dyes wastewater is determined by the expression [28]:

$$\text{Color removal (\%)} = \frac{\text{ABS}_0 - \text{ABS}_t}{\text{ABS}_0} \times 100 \quad (1)$$

where ABS<sub>0</sub> and ABS<sub>t</sub>, respectively, are the average absorbances before and after an electrolysis time *t* at the maximum visible wavelength (λ<sub>max</sub> = 520 nm) of the model dye, respectively.

The COD removal was calculated by the following formula [29]:

$$\text{COD removal} = \frac{\text{COD}_0 - \text{COD}_t}{\text{COD}_0} \times 100 \quad (2)$$

where COD<sub>0</sub> is the COD of initial concentration and COD<sub>t</sub> is the COD at given time *t*.

The current efficiency (CE, in %), expressed as a percentage, during Amaranth degradation process was defined as [30]:

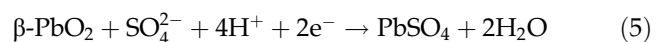
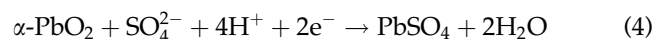
$$\text{CE} = \frac{(\text{COD}_0 - \text{COD}_t)}{8It} \times F \times V_s \times 100 \quad (3)$$

where COD<sub>0</sub> and COD<sub>t</sub> are the initial value before treatment and at time *t*, respectively, *F* is the Faraday constant (96,487 C mol<sup>-1</sup>), *V* is the volume of the electrolyte (L), and *I* is the average applied current (in A).

### 3. Results and discussion

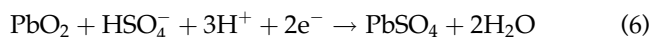
#### 3.1. Electrochemical behavior: cyclic voltammetry (CV)

The previous work confirmed that the lead oxide deposited film on stainless steel substrate is composed by α and β-PbO<sub>2</sub> forms [31]. It is reported in the literature [18], the ratio between α and β-PbO<sub>2</sub> modifications was changed by CV in sulfuric acid. The following reactions occur during cycling [32–34]:



Most of the α-PbO<sub>2</sub> and β-PbO<sub>2</sub> at the surface of the electrode are transformed into PbSO<sub>4</sub> owing to cathodic scan according to Eqs. (4) and (5); however, during the reverse scan, PbSO<sub>4</sub> is oxidized and gives preferably β-PbO<sub>2</sub>.

According to Carr and Hampson [35], the transformation of  $\text{PbSO}_4$  and  $\text{PbO}_2$  including the oxidation and reduction process can be given by the following reaction:



The CV measurements were performed in 0.5 M  $\text{H}_2\text{SO}_4$ . At the first voltammogram (Fig. 1(a)), we can show two clearly cathodic peaks, among them, the first one at 1.080 V and the second one at 1.158 V corresponding to the reduction of  $\beta$  and  $\alpha$ - $\text{PbO}_2$  into lead sulfate, respectively [20,28]. The anodic peak at potential of 1.830 V attributed to the oxidation of lead sulfate to  $\beta$ - $\text{PbO}_2$  form [19,36]. However, the reduction of  $\alpha$  form was fully disappeared after the fourth cycle (Fig. 1(c)), because the  $\alpha$ - $\text{PbO}_2$  structure is more difficult to be reduced to lead sulfate than  $\beta$  structure thanks its more compact structure so that only one reduced peak of  $\beta$  existed in slightly shifting to the left position [19,37]. Conversely, lead dioxide was formed in both forms with more  $\beta$  than  $\alpha$  form due to oxidation of lead sulfate during anodic process. But,  $\alpha$ -form was just formed from the tenth cycle at potential of 1.720 V. Otherwise, we can observe in (Fig. 1(d)–(f)) a rising of their redox peaks by cycle number.

### 3.2. Morphology and crystal structure of $\text{PbO}_2$ anodes

It has been previously reported [38,39] that the film  $\text{PbO}_2$  is electrodeposited from acidic solution as the tetragonal  $\beta$ -form, although a small amount of the orthorhombic  $\alpha$ -form is also existed depending on experimental conditions. It was found that the structural morphology of  $\text{PbO}_2$  using FESEM (Fig. 2) had different shapes and was changed and depended on the different cycle number of CV applied. At the first and second cycle of CV (Fig. 2(a) and (b)), the anodic layer consists of interconnected  $\text{PbSO}_4$  crystals, it can be seen at large magnifications that this layer consists of small grains or globules [32]. The small crystal of lead sulfate formed due to the reduction of  $\text{PbO}_2$ . The surface is more compact; as the morphology difference may not be due to the presence of both  $\alpha$  and  $\beta$  phases.

At the higher cycle number of CV, the  $\text{PbO}_2$  becomes porous due to oxygen bubbles on the surface during cycling process. The formed oxygen may cause cracks in the oxide structure and this in turn will result in a more porous oxide structure especially close to the surface [38].  $\text{PbSO}_4$  film is the first layer

formed in  $\text{PbO}_2$  anode that by which the in-depth porosity of the electrode may be destroyed [40]. Under this condition, the effect of CV on  $\text{PbO}_2$  film is confirmed and shown by the FESEM analysis (Fig. 2) demonstrated that no evidence of  $\text{PbSO}_4$  crystallites is visible after five CV.

### 3.3. Composition and structure

In order to obtain information about the structure and morphology of lead oxide film, Fig. 3 shows XRD pattern of  $\text{PbO}_2$  anodic layers before and after the cycling. It was found that  $\beta$ - $\text{PbO}_2$  form formed at  $2\theta$  degree equals to 62.2, 49.3, 46.2, 43.8, 25.6, 24.7, and 20.9, the  $\alpha$ - $\text{PbO}_2$  form was found at  $2\theta$  equals to 39.6, 37.5, 33.3, 29.8, and 23.5, while lead sulfate appeared at  $2\theta$  degree of 57.2, 55.6, 53.9, 53, 51, 44.8, 41.8, 32.4, 27.8, and 26.8 due to reduction of lead dioxide during the cycling process. These results were obtained to ASTM (American Metals Testing System) No 01-072-2440 and No 01-075-2417 and to the literature [19,41].

The change in the phase composition brought about by the cycle number of cyclic voltammetry (CV) was expressed by the change in the relative intensity of the reflections belonging to the phase,  $I_a/\sum I_n$ , where  $I_a$  denotes the intensity of the reflection belonging to the given phase and  $\sum I_n$  is the sum of the intensities of the characterization of reflections belonging to all phases [29].

For the investigation of CV behavior on the lead dioxide compounds, Fig. 4 illustrates the ratio of different compounds in anodic  $\text{PbO}_2$  layer with CV treatment. It was found that the ratio of  $\beta$ - $\text{PbO}_2/\text{PbSO}_4$  (Fig. 4(a)) decreased more quickly than that of  $\alpha$ - $\text{PbO}_2/\text{PbSO}_4$  (Fig. 4(b)) when cycle number of CV increased resulting to a quick decrease in the ratio between  $\beta$  and  $\alpha$  modifications also (Fig. 4(c)). This explained that the  $\beta$ - $\text{PbO}_2$  is favored process and attributed to incomplete reduction of  $\alpha$ - $\text{PbO}_2$  into  $\text{PbSO}_4$  oxidation of  $\text{PbSO}_4$ . However,  $\alpha$ - $\text{PbO}_2$  could be observed just from 10th cycle due to oxidation of  $\text{PbSO}_4$ .

Firstly, at the first cycle of CV, slow anodic reaction rate due to small corresponding current density was obtained because  $\text{PbO}_2$  existed already so that no oxidation process but only reduction of one of  $\text{PbO}_2$  into  $\text{PbSO}_4$  occurred. At higher cycle number of CV, beside the oxidation of  $\text{PbSO}_4$  into  $\text{PbO}_2$ ,  $\text{O}_2$  may be formed as a side reaction which can adsorb on the oxide layer and access into it resulting a more porous structure.

As soon as a passivating  $\text{PbSO}_4$  layer is formed on the surface, it plugs the pores and prevents further reaction, leaving an unreduced core of  $\text{PbSO}_4$ . For

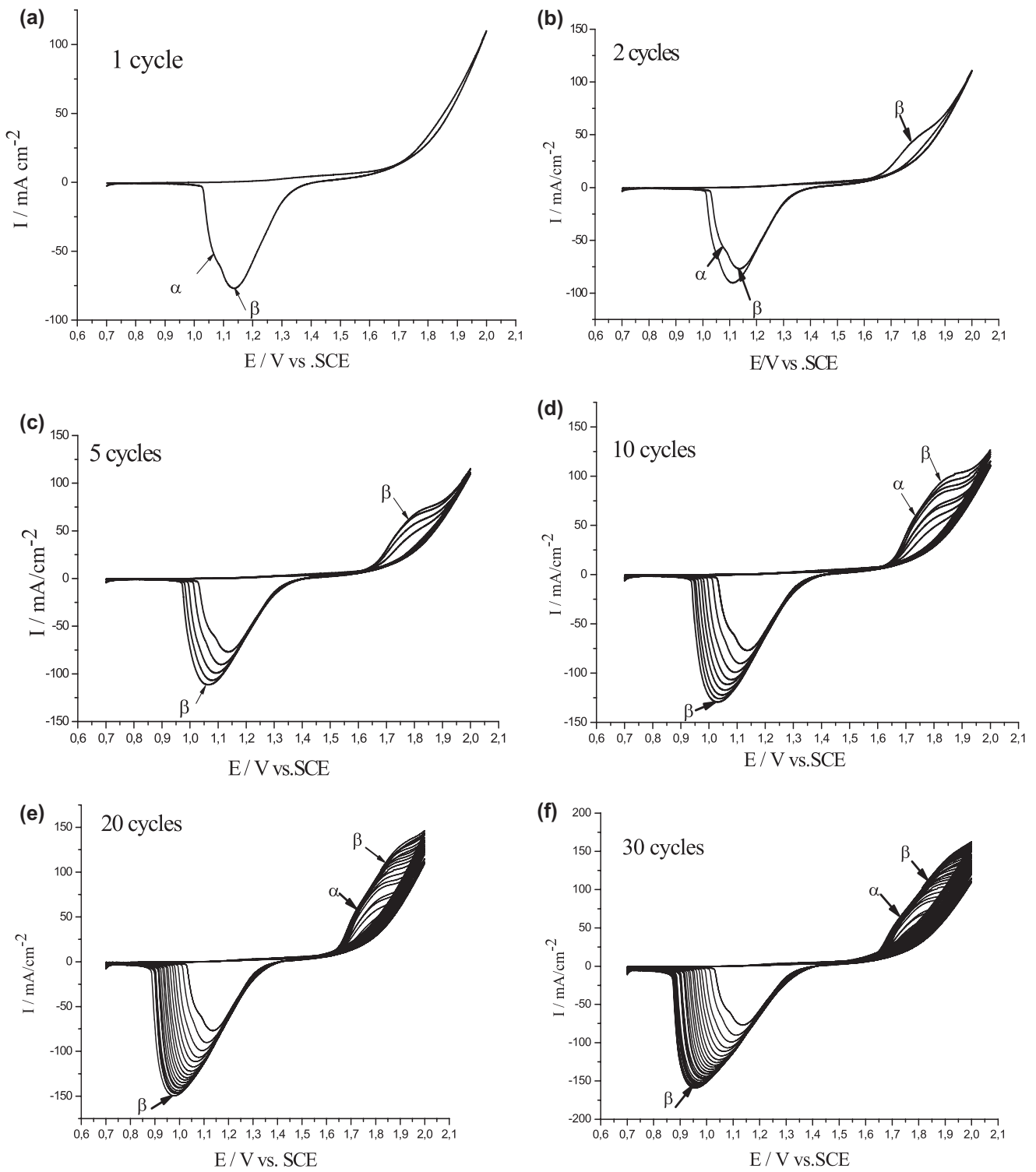


Fig. 1. Cyclic voltammograms of the prepared samples AS30/PbO<sub>2</sub> layer during (a) 1CV, (b) 2CV, (c) 5CV, (d) 10CV, (e) 20CV, and (f) 30CV in 0.5 M H<sub>2</sub>SO<sub>4</sub> at 50 mV s<sup>-1</sup>.

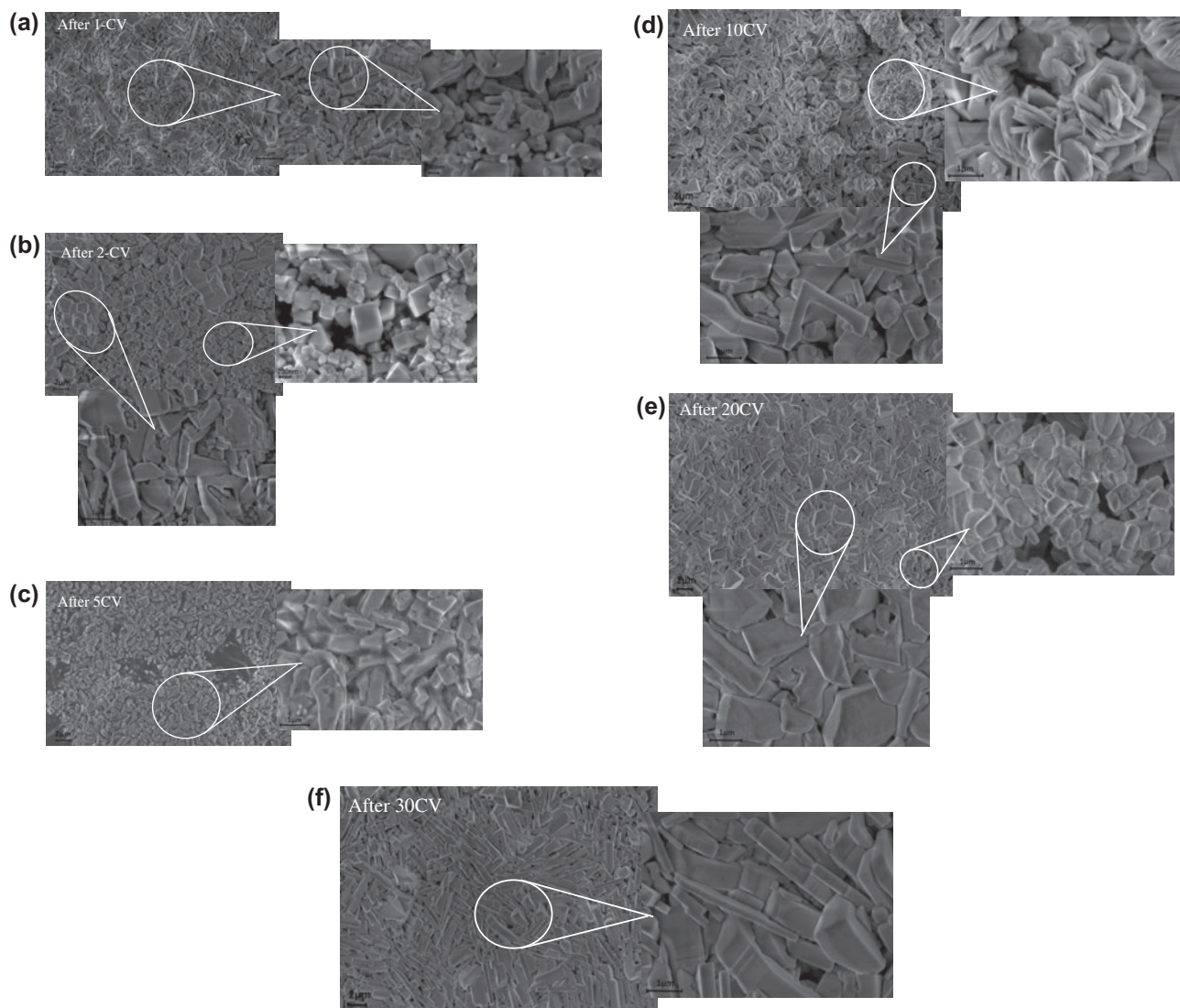


Fig. 2. FESEM images of the AS30/PbO<sub>2</sub> electrode (a) after 1st cycle, (b) after 2nd cycles, (c) 5th cycles, (d) 10th cycles, (e) 20th cycle, and (f) 30th cycles.

high current density value, the passivation reaction becomes faster due to the formation of much smaller PbSO<sub>4</sub> crystals, resulting in a higher degree of coverage [42].

Secondly, depending on the method used for preparation of the lead dioxide, the initial ratio of  $\alpha$ - and  $\beta$ -PbO<sub>2</sub> in a sample will vary, makes a loss of interparticle contact, and this is a problem since this contact is essential for good electrode performance. The percentage of  $\beta$ -PbO<sub>2</sub> form decreased when the number of cycle increased.

Finally, lead sulfate passivates the stainless steel surface and this indicates that the topography of the form layer has large impact on the properties.

### 3.4. Electrochemical impedance spectroscopy (EIS)

In order to investigate the effect of morphology and compounds of the prepared samples on the PbO<sub>2</sub> properties, EIS experiments were performed on the electrodes in 0.5 M H<sub>2</sub>SO<sub>4</sub> solution. Fig. 5(a) shows the Nyquist plots for different samples at open-circuit potential and 25°C. In order to obtain quantitative information, the Zsimpwin software considering the electric equivalent circuit used for data analysis shown in Fig. 5(b) containing six elements including a two-CPE model where CPE<sub>dl</sub> indicates the “Constant Phase Element related to double layer” of the interface and CPE<sub>f</sub> attributed to the film on stainless steel substrate,  $R_s$  corresponding to the electrolyte resistance,  $R_{ct}$  can

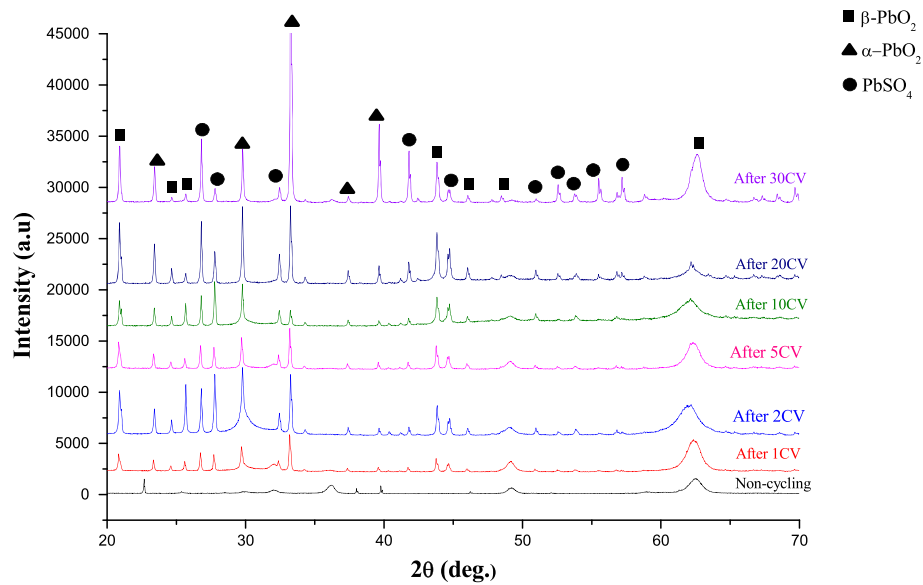


Fig. 3. XRD specters of AS30/PbO<sub>2</sub> electrode without and with different cycle number of CV applied.

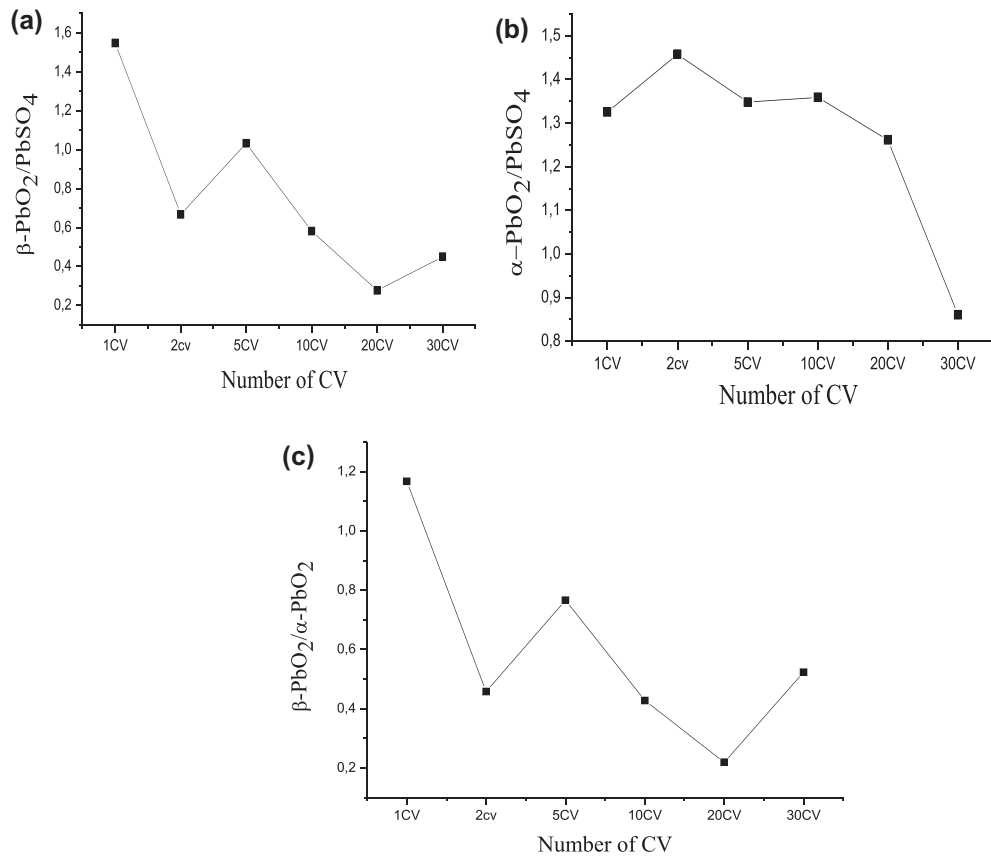


Fig. 4. The trend of the ratio related to (a)  $\beta\text{-PbO}_2/\text{PbSO}_4$  and (b)  $\alpha\text{-PbO}_2/\text{PbSO}_4$ , (c)  $\beta\text{-PbO}_2/\alpha\text{-PbO}_2$  forms as the function of CV cycle number.

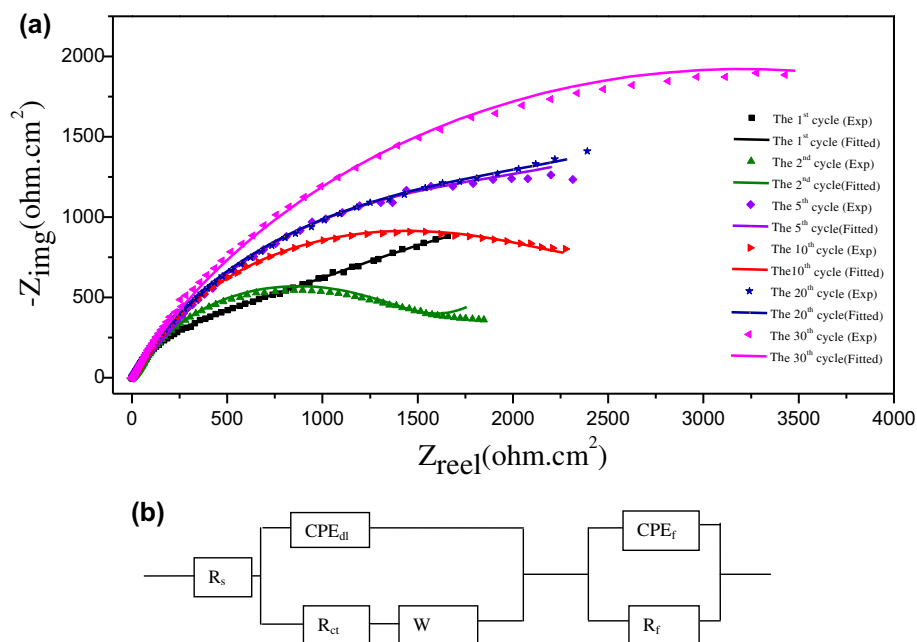


Fig. 5. (a) Nyquist plots of  $\text{PbO}_2$  film on stainless steel with different cycle number of CV applied and (b) the electric equivalent circuit used for fitting the experimental results.

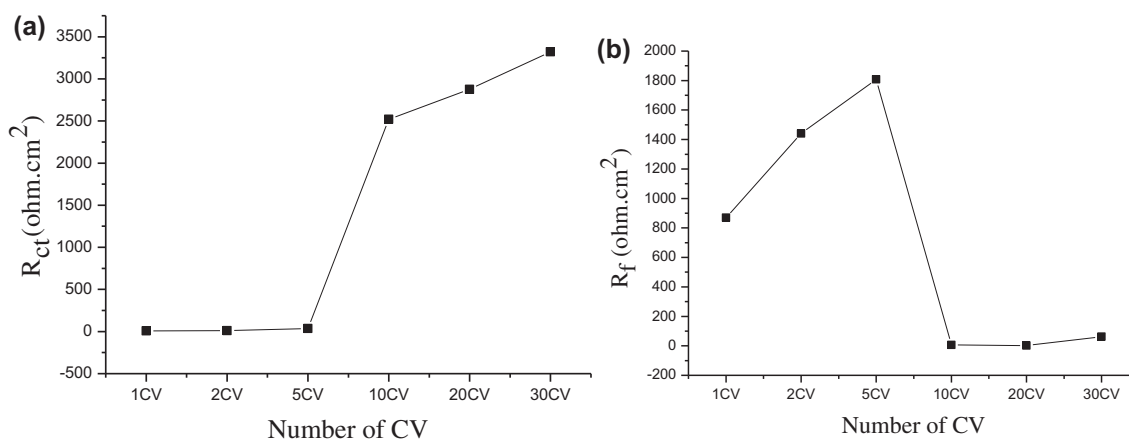


Fig. 6. Evolution of (a)  $R_{ct}$  and (b)  $R_f$  parameters during the CV applied.

describe the charge transfer resistance,  $R_f$  is the film resistance, and a finite length of Warburg impedance diffusion ( $W$ ).

As shown, in Fig. 5(a), the impedance spectra in Nyquist plots have a very strong dependence on the cycle number of CV applied on  $\text{PbO}_2$ . In fact, the plot obtained by the first cycle is different from the other plots after which this can be attributed to lead sulfate which acts strongly on the electrochemical behavior.

The  $R_{ct}$  values (Fig. 6(a)) are increased with increase in CV number which has an effect not only

on the morphology of the composite particles but also on the kinetic of the reaction. As it can be seen,  $R_{ct}$  for the  $\text{PbO}_2$  film at the first cycle is very small compared to that at the 30th one where the content of  $\text{PbSO}_4$  increased resulting to a reason for pore blocking in  $\text{PbO}_2$  with  $\text{PbSO}_4$  [43]. This process takes place at the level of the  $\text{PbSO}_4$  layer which is being seen as a semi-permeable precipitation membrane only for  $\text{H}^+$ ,  $\text{OH}^-$ , and  $\text{H}_2\text{O}$  species, but not for  $\text{SO}_4^{2-}$  ions [44].

The purpose of this study is to investigate the influence of the CV behavior on the adherence of the

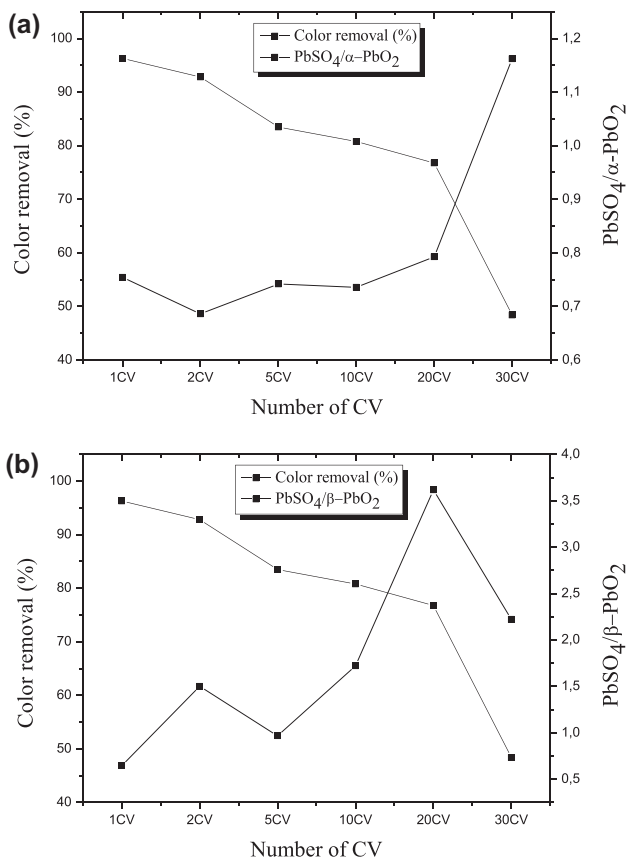


Fig. 7. The relationship between the color removal of Amaranth dye and the ration of PbSO<sub>4</sub>/α-PbO<sub>2</sub> and (b) PbSO<sub>4</sub>/β-PbO<sub>2</sub>.

PbO<sub>2</sub> film comparing to that without CV treatment in our previous study where we have detachment throughout the anodic oxidation of pollutant model.

However, the resistance of PbO<sub>2</sub> film in 0.5 M H<sub>2</sub>SO<sub>4</sub> (Fig. 6(b)) becomes more resistive especially for the first five cycles of CV applied on pulsed PbO<sub>2</sub> film, due to its composition. According to CV behavior, even we cannot observe the peak corresponding

to the oxidation of PbSO<sub>4</sub> to α-PbO<sub>2</sub>. According to our previous work [31], when we have AS30/PbO<sub>2</sub> anode without CV treatment, it was absence of PbSO<sub>4</sub> form and therefore a problem of detachment of PbO<sub>2</sub> film is observed, also the  $R_f$  value in the order to 5.47 Ω cm<sup>2</sup>. In the case of CV treatment, the presence of PbSO<sub>4</sub> protects the stainless steel substrate and this can be a reason for the adherence of lead oxide during anodic oxidation process.

### 3.5. Anodic oxidation of Amaranth

The effect of CV was evaluated by the degradation experiments of Amaranth dye. Zerroual et al. [45] extensively studied the relationship between the structures on PbO<sub>2</sub> and generation of OH<sup>•</sup>. They proposed a mechanism accounting for the electrochemical processes taking place on the lead dioxide electrode. As we know, the formation of hydroxyl radicals from the discharge of water molecules on the surface of lead dioxide anode.

Lead dioxide exists in low crystalline forms: α (orthorhombic) and β (tetragonal); α-PbO<sub>2</sub> has a lower oxygen evolution over potential than that of β-PbO<sub>2</sub> [46]. Consequently, β-PbO<sub>2</sub> must logically be more efficient for the degradation of organic compounds than α-PbO<sub>2</sub>. In fact, it has been proven that the electrocatalytic activity of a PbO<sub>2</sub> deposit depends on its chemical composition and on its crystalline structure [47]. Depending on the preparation conditions of the PbO<sub>2</sub> deposit, there can be either a mixture of both forms α and β or one of them only [48]. The proportion of α and β in this mixture mainly depends on the anodic oxidation density of PbO<sub>2</sub> electro-deposition [49]. Parallel to electro-deposition of PbO<sub>2</sub>, oxygen evolution inevitably occurs at the electrode surface. The rate of PbO<sub>2</sub> formation and consequently its structure must thus depend on the oxygen over-potential of the substrate on which it is supported.

Table 1

Amaranth dye discoloration and mineralization kinetic of PbO<sub>2</sub> with and without CV on stainless steel (AS30) after 5 h electrolysis for  $\lambda = 520$  nm. The  $K_{app}$  is the kinetic value according pseudo first order

AS30/PbO <sub>2</sub>	$K_{app}$ dis ( $10^{-3} \text{ min}^{-1}$ )	$R^2$	$K_{app}$ COD ( $10^{-3} \text{ min}^{-1}$ )	$R^2$
1CV	4.30	0.97	5.75	0.99
2CV	3.92	0.97	5	0.99
5CV	2.03	0.97	4.32	0.99
10CV	3.80	0.98	3.90	0.99
20CV	3.49	0.99	3.43	0.98
30CV	3.59	0.98	1.76	0.97

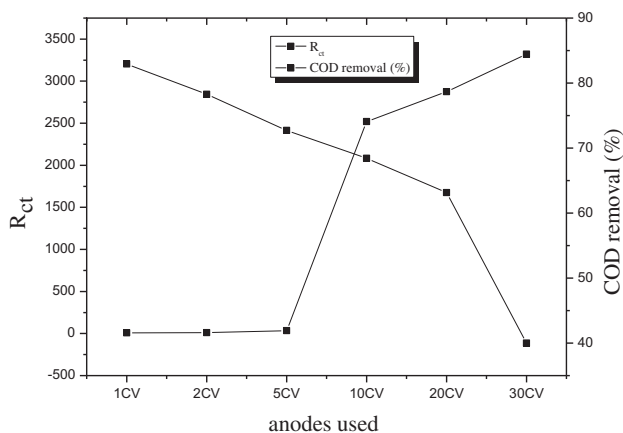


Fig. 8. COD removal and  $R_{ct}$  of Amaranth E123 during the oxidation on different anodes used, operation conditions:  $C_0E123$ , 0.015 mM;  $T$ , 25°C; applied current density, 25 mA cm<sup>-2</sup>; pH 2.

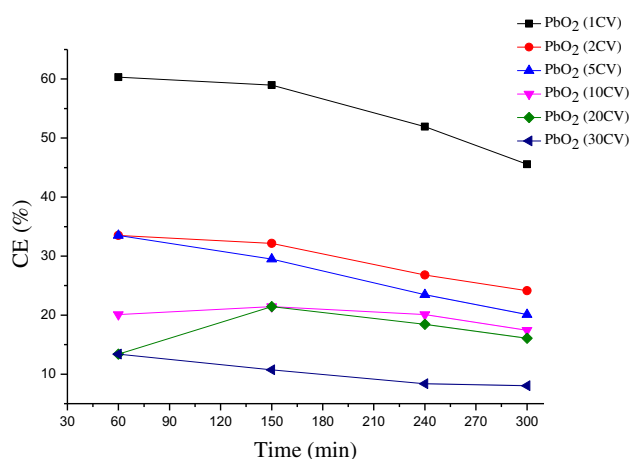


Fig. 9. Evolution of current efficiency (CE) with electrolysis time. Operation conditions  $C_0E123$ , 0.015 mM;  $T$ , 25°C; applied current density, 25 mA cm<sup>2</sup>; pH 2.

The color removal of Amaranth dye on AS30/PbO<sub>2</sub> with different number of CV applied is shown in Fig. 7

explained that the color removal reached nearly 97, 93, 84, 80, 78, 77, and 49% for anodes treated by 1, 2, 3, 5, 10, 20, and 30 CV, respectively.

According to DRX analysis, the ratio of lead sulfate increased with the increase in number of CV and the efficiency of AS30/PbO<sub>2</sub> electrodes in Amaranth degradation as a function of cyclic number is probably due to a blockage of certain of its electro-catalytic sites by the lead sulfate participate and the formation of  $\alpha$ -PbO<sub>2</sub> characterized by low O<sub>2</sub> evolution. By increasing the PbSO<sub>4</sub> ratio in the PbO<sub>2</sub> electrode, some sulfate ions were converted yielding the inhibition of the electrochemical performance of the electrode AS30/PbO<sub>2</sub> [50]. The presence of  $\beta$ -form must be logically being more efficient for degradation of organic compounds than  $\alpha$ -PbO<sub>2</sub> because of its higher oxygen evolution overpotential [51].

Electrolysis of Amaranth was carried out, under the same operating conditions using all anodes. The parameters of the kinetics of all anodes used as summarized in Table 1, we can observe the highest  $k_{app}$  value for AS30/PbO<sub>2</sub> with one CV.

In order to study the influence of the content of different crystal forms in PbO<sub>2</sub> film formed after CV treatment of surface in the electrolysis, the comparison of the COD removal during the oxidation with different anodes was performed (Fig. 8) which reflects the global mineralization of initial pollutant and its by-products. It was observed that the change in the ratio between different crystal forms (mainly lead sulfate form) has influence on oxidation rate. This influence is seen in COD removal, where AS30/PbO<sub>2</sub> anode treated with 1, 2, 5, 10, 20, and 30 CV reached the COD removals of about 83, 78, 73, 68, 63, 40 and 47%, respectively. Comparing the value of  $R_{ct}$ , we could find out a relationship between it with COD removal. For instance, the PbO<sub>2</sub> treated by one CV cycle displayed the smallest  $R_{ct}$  that resulted to the highest COD removal percentage. However, with 30 CV possessed the largest  $R_{ct}$  which may be a reason for the lowest removal efficiency. The  $\beta$ -form presenting more porous structure can act on the semi conductor

Table 2

Concentration of Pb<sup>2+</sup> (mg L<sup>-1</sup>) in solution samples after different electrolysis times

Tim (min)	AS30/PbO <sub>2</sub>	1 cycle	The 2nd cycle	The 5th cycle	The 10th cycle	The 20th cycle	The 30th cycle
0	0	0	0	0	0	0	0
60	0.356	0	0	0	0	0	0
90	0.423	0	0	0	0	0	0
150	1.342	0.044	0.081	0.096	0.128	0.204	0.361
240	1.489	0.189	0.267	0.303	0.486	0.495	0.501

properties with the possibility of more ability for electron moving (semi conductor type n).

Fig. 9 shows the variation of current efficiency (CE) during electrolysis time used to decolorize Amaranth dye for all anodes is used. It is clear that the decrease in CV behavior can increase the CE values of PbO<sub>2</sub>. Electrode among the lowest and highest one was obtained by 30 CV and 1 CV, respectively, contrast, the PbO<sub>2</sub> (1CV) electrode has highest CE removal.

### 3.6. Atomic absorption

After electrolysis time, all samples were analyzed with GFAAS to determinate the trace amounts of lead ion in solution. Table 2 summarized the concentration of Pb<sup>2+</sup> in solutions during electrolysis time for all anodes used under degradation of Amaranth dye. When we use the AS30/PbO<sub>2</sub> anode treated by one CV, we can observe that the Pb<sup>2+</sup> concentration was the smaller compared to ather CV applied. We can conclude that it has an effect on the adherence of PbO<sub>2</sub> film.

## 4. Conclusions

PbO<sub>2</sub> anodic layers were formed by pulsed method in attempt to study PbO<sub>2</sub> processed with different CV cycle number as anode for degradation dye. The structural and electrochemical properties of PbO<sub>2</sub> anodic layers treated by CV were examined and found to be different. Comparatives studies indicate that the effect of cyclic voltammetry exhibited more performance of oxide layer on stainless steel. Through FESEM observation, it was established that the influence of CV behavior on morphology forms and the X-ray analyses demonstrated the presence of PbSO<sub>4</sub> layer and their content increases throughout the increase in CV cycle number. The prepared electrodes were subjected to various electrochemical measurements including CV and EIS in acidic media. The results indicate that the peak from reduction of  $\alpha$ -PbO<sub>2</sub> to PbSO<sub>4</sub> disappeared after the fifth cycle of CV. EIS results revealed that the charge-transfer resistance significantly decreased because the presence of lead sulfate layer blocked the access of electrolyte ions to the internal layer. The resistance of the film increases during the first five cyclic voltammetry and this result can be attributed to the presence of PbSO<sub>4</sub> layer.

It was concluded that the CV treatment improves the adherence of PbO<sub>2</sub> on stainless steel substrate. The color and COD values were obtained around 97 and 83%, respectively, using SS/PbO<sub>2</sub> anode with 1st anode

treated by only one CV cycle and thus it could be applied in large scale in wastewater treatment.

## Acknowledgment

This research is carried out with the support of International Foundation for Science (IFS), Sweden, by a research fellowship to CP: Hanene Akrouit–Baccour.

## References

- [1] J.M. Aquino, R.C. Rocha-Filho, N. Bocchi, S.R. Biaggio, Electrochemical degradation of the Disperse Orange 29 dye on a  $\beta$ -PbO<sub>2</sub> anode assessed by the response surface methodology, *J. Environ. Chem. Eng.* 1 (2013) 954–961.
- [2] M. Hamza, S. Ammar, R. Abdelhédi, Electrochemical oxidation of 1,3,5- trimethoxybenzene in aqueous solutions at gold oxide and lead dioxide electrodes, *Electrochim. Acta* 56 (2011) 3785–3789.
- [3] G.K. Ramesha, S. Sampath, In-situ formation of graphene–lead oxide composite and its use in trace arsenic detection, *Sens. Actuators B: Chem.* 160 (2011) 306–311.
- [4] D.R.P. Egan, C.T.J. Low, F.C. Walsh, Electrodeposited nanostructured lead dioxide as a thin film electrode for a lightweight lead-acid battery, *J. Power Sources* 196 (2011) 5725–5730.
- [5] P. Perret, Z. Khani, T. Brousse, D. Bélanger, D. Guay, Carbon/PbO<sub>2</sub> asymmetric electrochemical capacitor based on methanesulfonic acid electrolyte, *Electrochim. Acta* 56 (2011) 8122–8128.
- [6] I. Elaiassaoui, H. Akrouit, L. atifa Bousselmi, Electrochemical Behavior of lead dioxide electrodeposited on different substrate: Lead and stainless steel, the 3rd International Colloquium on Materials Corrosion and their Protection CMP12, 05–08 Decembere, Tunisia, 2012.
- [7] J. Morales, G. Petkova, M. Cruz, A. Caballero, Synthesis and characterization of lead dioxide active material for lead-acid batteries, *J. Power Sources* 158 (2006) 831–836.
- [8] S. Ghasemi, M.F. Mousavi, M. Shamsipur, H. Karami, Sonochemical-assisted synthesis of nano-structured lead dioxide, *Ultrason. Sonochem.* 15 (2008) 448–455.
- [9] H.S. Kong, W. Li, H. Lin, Z. Shi, H. Lu, Y. Dan, W. Huang, Influence of F-doping on the microstructure, surface morphology and electrochemical properties of the lead dioxide electrode, *Surf. Interface Anal.* 45 (2013) 715–721.
- [10] A.B. Velichenko, R. Amadelli, E.V. Gruzdeva, T.V. Luk'yanenko, F.I. Danilov, Electrodeposition of lead dioxide from methanesulfonate solutions, *J. Power Sources* 191 (2009) 103–110.
- [11] P.K. Shen, X.L. Wei, Morphologic study of electrochemically formed lead dioxide, *Electrochim. Acta* 48 (2003) 1743–1747.
- [12] S. Ghasemi, H. Karami, M.F. Mousavi, M. Shamsipur, Synthesis and morphological investigation of pulsed current formed nano-structured lead dioxide, *Electrochim. Commun.* 7 (2005) 1257–1264.
- [13] A. Sharma, S. Bhattacharya, R. Sen, B.S.B. Reddy, H.-J. Fecht, K. Das, S. Das, Influence of current density on

- microstructure of pulse electrodeposited tin coatings, *Mater. Charact.* 68 (2012) 22–32.
- [14] I. Sirés, C.T.J. Low, C. Ponce-de-León, F.C. Walsh, The characterisation of PbO<sub>2</sub>-coated electrodes prepared from aqueous methanesulfonic acid under controlled deposition conditions, *Electrochim. Acta* 55 (2010) 2163–2172.
- [15] N. Yu, L. Gao, S. Zhao, Z. Wang, Electrodeposited PbO<sub>2</sub> thin film as positive electrode in PbO<sub>2</sub>/AC hybrid capacitor, *Electrochim. Acta* 54 (2009) 3835–3841.
- [16] H. Karami, B. Kafi, M. Sayed Najmmadin, Effect of particle size on the cyclic voltammetry parameters of nanostructured Lead dioxide, *Int. J. Electrochem. Sci.* 4 (2008) 414–424.
- [17] J. Wang, X. Li, L. Guo, X. Luo, Effect of surface morphology of lead dioxide particles on their ozone generating performance, *Appl. Surf. Sci.* 254 (2008) 6666–6670.
- [18] I. Petersson, E. Ahlberg, B. Berghult, Parameters influencing the ratio between electrochemically formed  $\alpha$ - and  $\beta$ -PbO<sub>2</sub>, *J. Power Sources* 76 (1998) 98–105.
- [19] D. Zhou, L. Gao, Effect of electrochemical preparation methods on structure and properties of PbO<sub>2</sub> anodic layer, *Electrochim. Acta* 53 (2007) 2060–2064.
- [20] M. Ghaemi, E. Ghafouri, J. Neshati, Influence of the nonionic surfactant Triton X-100 on electrocrystallization and electrochemical performance of lead dioxide electrode, *J. Power Sources* 157 (2006) 550–562.
- [21] Y. Zheng, W. Su, S. Chen, X. Wu, X. Chen, Ti/SnO<sub>2</sub>-Sb<sub>2</sub>O<sub>5</sub>-RuO<sub>2</sub>/ $\alpha$ -PbO<sub>2</sub>/ $\beta$ -PbO<sub>2</sub> electrodes for pollutants degradation, *Chem. Eng. J.* 174 (2011) 304–309.
- [22] J.M. Aquino, R.C. Rocha-Filho, L.A.M. Ruotolo, N. Bocchi, S.R. Biaggio, Electrochemical degradation of a real textile wastewater using  $\beta$ -PbO<sub>2</sub> and DSA<sup>®</sup> anodes, *Chem. Eng. J.* 251 (2014) 138–145.
- [23] D. Pavlov, A. Dakhouche, T. Rogachev, Influence of antimony ions and PbSO<sub>4</sub> content in the corrosion layer on the properties of the grid/active mass interface in positive lead-acid battery plates, *J. Appl. Electrochem.* 27 (1997) 720–730.
- [24] V. Suryanarayanan, I. Nakazawa, S. Yoshihara, T. Shirakashi, The influence of electrolyte media on the deposition/dissolution of lead dioxide on boron-doped diamond electrode—A surface morphologic study, *J. Electroanal. Chem.* 592 (2006) 175–182.
- [25] Y. Yao, M. Zhao, C. Zhao, H. Zhang, Preparation and properties of PbO<sub>2</sub>-ZrO<sub>2</sub> nanocomposite electrodes by pulse electrodeposition, *Electrochim. Acta* 117 (2014) 453–459.
- [26] M.N. Naim, M. Kuwata, H. Kamiya, I. Lenggoro, Deposition of TiO<sub>2</sub> nanoparticles in surfactant-containing aqueous suspension by a pulsed DC charging-mode electrophoresis, *J. Ceram. Soc. Jpn.* 117 (2009) 127–132.
- [27] P.T. Binh, M.T.T. Thuy, Characterization of PbO<sub>2</sub> synthesized by current pulse method on stainless steel, *J. Chem.* 47(5A) (2009) 60–64.
- [28] Y. Liu, H. Liu, J. Ma, J. Li, Investigation on electrochemical properties of cerium doped lead dioxide anode and application for elimination of nitrophenol, *Electrochim. Acta* 56 (2011) 1352–1360.
- [29] W.P.B. Barros, J.R. Steter, M.R.V. Lanza, A.J. Motheo, Degradation of amaranth dye in alkaline medium by ultrasonic cavitation coupled with electrochemical oxidation using a boron-doped diamond anode, *Electrochim. Acta* 143 (2014) 180–187.
- [30] K.T. Kawagoe, D.C. Johnson, Electrocatalysis of anodic oxygen-transfer reactions oxidation of phenol and benzene at bismuth-doped lead dioxide electrodes in acidic solution, *J. Electrochem. Soc.* 141 (1994) 3404–3409.
- [31] I. Elaiassaoui, H. Akrouf, L. Bousselmi, Interface behavior of PbO<sub>2</sub> on pure lead and stainless steel as anode for dye degradation, *Desalin. Water Treat.* (2015), doi: 10.1080/19443994.2015.1079250.
- [32] P. Casson, N.A. Hampson, K. Peters, P. Whyatt, An investigation of the surface structure of some lead dioxide and related electrodes, *J. Appl. Electrochem.* 7 (1977) 257–265.
- [33] H. Nguyen, P. Cong, Chartier, Electrodeposited  $\alpha$ -PbO<sub>2</sub> and  $\beta$ -PbO<sub>2</sub> in sulfuric acid: Recharge, cycling and morphology, *J. Power Sources* 13 (1984) 223–233.
- [34] D. Devilliers, M.T. Dinh Thi, E. Mahe, V. Dauriac, N. Lequeux, Electroanalytical investigations on electrodeposited lead dioxide, *J. Electroanal. Chem.* 573 (2004) 227–239.
- [35] J.P. Carr, N.A. Hampson, Lead dioxide electrode, *Chem. Rev.* 72 (1972) 679–703.
- [36] H. Karami, B. Kafi, S.N. Mortazavi, Effect of particle size on the cyclic voltammetry parameters of nanostructured lead dioxide, *Int. J. Electrochem. Sci.* 4 (2009) 414–424.
- [37] H. Karami, A. Yaghoobi, A. Ramazani, Sodium sulfate effects on the electrochemical behaviors of nanostructured lead dioxide and commercial positive plates of lead-acid batteries, *Int. J. Electrochem. Sci.* 5 (2010) 1046–1059.
- [38] N. Munichandraiah, Physicochemical properties of electrodeposited-lead dioxide: Effect of deposition current density, *J. Appl. Electrochem.* 22 (1992) 825–829.
- [39] N. Vatisstas, S. Cristofaro, Lead dioxide coating obtained by pulsed current technique, *Electrochem. Commun.* 2 (2000) 334–337.
- [40] C. Lazarides, N.A. Hampson, The impedance of a planté PbO<sub>2</sub> electrode polarized in H<sub>2</sub>SO<sub>4</sub> solution, *Surface Technol.* 17 (1982) 139–146.
- [41] N. Mohammadi, M. Yari, S.R. Allahkaram, Characterization of PbO<sub>2</sub> coating electrodeposited onto stainless steel 316L substrate for using as PEMFC's bipolar plates, *Surf. Coat. Technol.* 236 (2013) 341–346.
- [42] Z. Yao, Z. Jiang, F. Wang, Study on corrosion resistance and roughness of micro-plasma oxidation ceramic coatings on Ti alloy by EIS technique, *Electrochim. Acta* 52 (2007) 4539–4546.
- [43] J.A. Bialacki, N.A. Hampson, The A.C. impedance of porous PbO<sub>2</sub> on a lead support in sulphuric acid, *Surf. Technol.* 23 (1984) 117–125.
- [44] P. Rüetschi, Influence of crystal structure and interparticle contact on the capacity of PbO<sub>2</sub> electrodes, *J. Electrochem. Soc.* 139 (1992) 1347–1351.
- [45] L. Zerroual, R. Fitas, B. Djellouli, N. Chelali, Relationship between water departure and capacity loss of  $\alpha$  and  $\beta$ -PbO<sub>2</sub> using an all solid-state system: Estimation of proton diffusion coefficient, *J. Power Sources* 158 (2006) 837–840.
- [46] C. Tan, B. Xiang, Y. Li, J. Fang, M. Huang, Preparation and characteristics of a nano-PbO<sub>2</sub> anode for organic wastewater treatment, *Chem. Eng. J.* 166 (2011) 15–21.
- [47] F.J. Recio, P. Herrasti, I. Sirés, A.N. Kulak, D.V. Bavykin, C. Ponce-de-León, F.C. Walsh, The

- preparation of  $\text{PbO}_2$  coatings on reticulated vitreous carbon for the electro-oxidation of organic pollutants, *Electrochim. Acta* 56 (2011) 5158–5165.
- [48] H. Yang, B. Chen, Z. Guo, H. Liu, Y. Zhang, H. Huang, R. Xu, R. Fu, Effects of current density on preparation and performance of Al/conductive coating/ $\alpha\text{-PbO}_2\text{-CeO}_2\text{-TiO}_2/\beta\text{-PbO}_2\text{-MnO}_2\text{-WC-ZrO}_2$  composite electrode materials, *Trans. Nonferr. Met. Soc. China* 24 (2014) 3394–3404.
- [49] F. Chen, S. Yu, X. Dong, L. Zhang, Q. Wu, Preparation and characterization of  $\text{PbO}_2$  electrode and its application in electro-catalytic degradation of o-aminophenol in aqueous solution assisted by  $\text{CuO-Ce}_2\text{O}_3/\delta\text{-Al}_2\text{O}_3$  catalyst, *J. Hazard. Mater.* 260 (2013) 747–753.
- [50] M. Foudia, M. Matrakova, L. Zerroual,  $\text{PbSO}_4$  as a precursor for positive active material electrodes, *J. Power Sources* 207 (2012) 51–55.
- [51] S. Rada, L. Rus, M. Rada, E. Culea, N. Aldea, Synthesis, structure, optical and electrochemical properties of the lead sulfate-lead dioxide-lead glasses and vitroceramics, *Solid State Ionics* 274 (2015) 111–118.